

Strengthening in MgLi matrix composites reinforced with unidirectional T300 and Granoc carbon fibres

S. Kúdela Jr.^{1*}, O. Bajana¹, Ľ. Orovčík¹, P. Ranachowski², Z. Ranachowski²

¹*Institute of Materials & Machine Mechanics, Slovak Academy of Sciences,
Dúbravská cesta 9, 845 13 Bratislava, Slovak Republic*

²*Institute of Fundamental Technological Research, Polish Academy of Sciences,
Pawinskiego 5B, 02-106 Warszawa, Poland*

Received 18 November 2019, received in revised form 16 December 2019, accepted 16 December 2019

Abstract

Mg-2 wt.% Li matrix composites unidirectionally reinforced with T300 and Granoc carbon fibres (~ 45 vol.%) were prepared by the gas pressure infiltration technique. Lithium alloying stimulates the interfacial bond formation and at the same time causes the damage of carbon fibres by Li₂C₂ formation. Auger electron spectroscopy was used to detect Li₂C₂ inside the carbon fibres. The maximum flexural strength (1210 MPa) was achieved in Mg₂Li/T300 composites at the shortest infiltration time (5 s) and then decreased monotonously with infiltration time prolongation (up to 60 s). Strengthening in Mg₂Li/Granoc composites was much lower when maximum bending strength of 579 MPa was reached.

Key words: magnesium composites, magnesium-lithium composites, T300 carbon fibres, Granoc carbon fibres, lithium carbide, reactive wetting

1. Introduction

Key parameters influencing the mechanical performance of metal matrix composites are fibre volume fraction, fibre architecture and interfacial bonding. The latter factor is quite frequently ignored since, in almost all models, the interface between the matrix and the fibres is a priori considered sufficiently strong without interfacial failure. In praxis, various experimental methods are applied to overcome the difficulties concerning the interfaces. An essential requirement for good fibre–matrix bond is good wetting. A direct relationship exists between the wettability of fibres by molten metals and interfacial bonding [1]. In principle, there are two techniques to solve this problem: the coating of reinforcing fibres and the matrix alloying. The economically and technologically more appropriate alternative appears to be the matrix alloying.

When focusing on magnesium-based composites, their strengthening with advanced carbon fibres is an attractive idea as the resultant products potentially exhibit excellent specific strength and/or stiff-

ness. These composites are usually fabricated by the melt infiltration of the fibrous preform. The non-reactive character of the system C/Mg, however, leads to poor wetting and thus very weak interfacial bonding. In principle, this problem can be solved by alloying of magnesium matrix with a carbide-forming element, typically Al, which forms Al₄C₃ and Al₂MgC₂ carbides that significantly improve the interfacial strength [2]. These carbides nucleate and grow on the surface of carbon fibres which, however, affects their structure and reduces sharply resultant strengthening [3].

Promising results have recently been reported concerning the alloying of magnesium matrix with rare earth elements Y and Gd [4, 5]. The composites were fabricated by the melt infiltration under atmospheric conditions. In both cases, Y or Gd segregated at interfaces forming fine particles Mg₂Y, Mg₂₄Y₅, Mg₇Gd, and oxidic layers Gd₂O₃ and MgO. As a result, the interfacial strength, as determined by interfacial shear stress (ISS) test, has greatly been enhanced. It is, however, noteworthy that the author did not mention any carbidic phase, although both Y and Gd exhibit high

*Corresponding author: tel.: +421 2 32401029; e-mail address: ummskudm@savba.sk

Table 1. Basic data on carbon fibres T300 [7] and Granoc [8]

Carbon fibre (Producer)	Fibre type	Young's modulus (GPa)	Tensile strength (GPa)	Density (g cm^{-3})	Diameter (μm)
Torayca T300 (Toray)	PAN	230	3.53	1.76	7
Granoc XN90-60S (Nippon Graphite)	Pitch	860	3.50	2.20	10

potential for forming YC₂ and GdC₂ carbides, respectively. Maybe it is a new approach that enables to prevent from the detrimental effect of carbidic products on the strengthening efficiency of carbon fibres.

Alloying of Mg matrix with Li initiates reactive wetting of carbon fibres, thus facilitating the formation of the interfacial bond [6]. In the present study, there are tested PAN-based fibres T300 (Toray) and pitch-based Granoc ones (Nippon Graphite) as reinforcements of Mg-2 wt.% Li matrix. Carbon fibres tested differ in their reactivities which significantly influences the formation of interfaces. The structure of PAN-based T300 fibres consists of turbostratic graphite with disordered small graphene-like blocks. In contrast, the structure of pitch-based Granoc fibres consists of large graphene layers with aligned orientation [7]. As a result, T300 fibres exhibit higher reactivity due to their low crystalline structure containing a large number of edge carbon atoms as active centres for chemical reactions. On the contrary, higher crystallinity of Granoc fibres generates much less edge carbon atoms so that they are expected to be more resistant to molten MgLi alloys than T300 ones. Different reactivity of carbon fibres influences the formation of interfacial bond in fabricated MgLi matrix composites, thus having a crucial impact on resultant composite strengthening.

2. Experiment

2.1. Mg-Li alloy preparation

Magnesium-lithium matrix alloys with nominal lithium alloying of 2 wt.% Li marked further as Mg₂Li have been prepared by fusion of pure magnesium (purity of 99.9%, LMT Metalurgie) and lithium (purity of 99.0%, Merck) in a mild-steel crucible followed with casting into a cylindrical steel mould. Both fusion and casting operations were conducted in the same chamber under an argon pressure of 1 MPa after the previous evacuation (10 Pa).

2.2. Composite fabrication

Mg₂Li/T300 and Mg₂Li/Granoc composite samples were fabricated by infiltration of PAN-based carbon fibres Torayca T300 (Toray) and pitch-based carbon fibres Granoc XN90-60S (Nippon Graphite) with

molten Mg₂Li matrix alloy. Primary data on T300 and Granoc carbon fibres are listed in Table 1 [8, 9]. The melt infiltration was carried out by the vacuum – pressure technique in labour autoclave. Preheated fibrous preform ($15 \times 15 \times 70 \text{ mm}^3$) made of perforated steel sheet with unidirectionally arranged T300 carbon fibres ($\sim 45 \text{ vol.}\%$) was immersed under vacuum ($\leq 10 \text{ Pa}$) into molten Mg₂Li alloy at 700 °C. Then the argon pressure of 4 MPa was applied for 5, 15, 30, and 60 s. The preform with infiltrated carbon fibres was subsequently withdrawn from molten metal under argon pressure and cooled down. Infiltration of Granoc carbon fibres ($\sim 45 \text{ vol.}\%$) was conducted in the same way at temperatures of 750 °C and 850 °C for 30 and 60 s. For comparison, there were also prepared Mg/T300 and Mg/Granoc composites at 750 °C/60 s using the same fabrication procedure.

2.3. Auger electron spectroscopy

Auger electron spectra were acquired gradually from the central part of selected carbon fibre cross-section in combination with sputtering (Ar + ions, 4 keV/125 $\mu\text{A cm}^{-2}$) to gain the spectra depth profiles. The spectra were recorded at 10 keV/10 nA using Perkin Elmer PHI 660 SAM apparatus and treated by Savitzky-Golay 5-point differentiation. Before performing the Auger analysis itself, the sample was slightly pre-sputtered. The measurements have been performed at IFW Dresden.

2.4. SEM observations and EDX analysis

The structure of MgLi/CF and composites was examined using the scanning electron microscope (SEM, Jeol JSM 7600F) equipped with retractable backscattered electron detector (RBEI). Energy-dispersive X-ray spectrometer (EDX) operating at 15 kV was used for elemental analysis. Composite samples were metallographically polished using water-free isopropyl alcohol to a mirror-like finish without any etching. As the structure of MgLi/CF composites is sensitive to atmospheric humidity, they were exposed to air for a limited time ($\leq 1 \text{ h}$) before being SEM and EDX inspected.

2.5. Bending tests

The bending strength has been chosen as a crite-

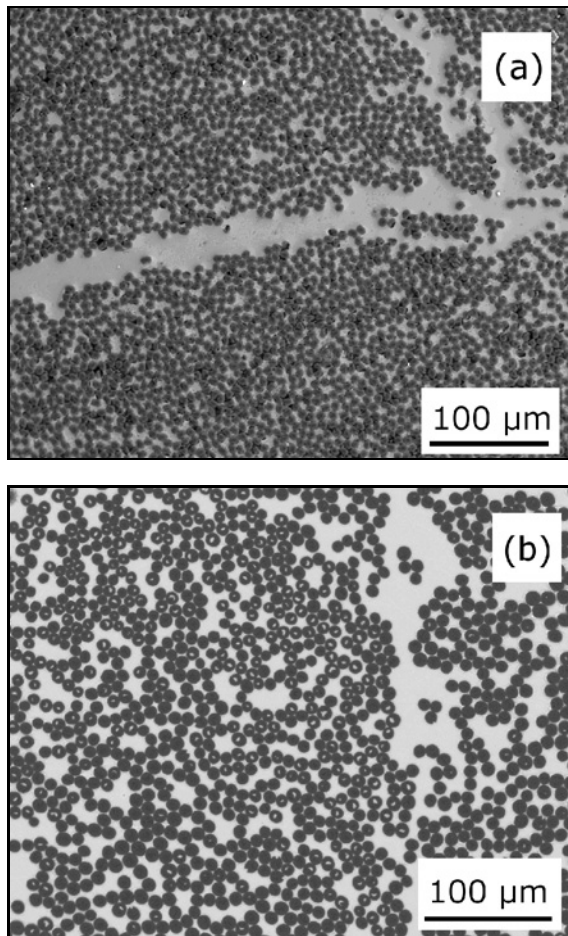


Fig. 1. Overall structure of Mg₂Li/T300 (a) and Mg₂Li/GRANOC (b) composites (SEM).

tion of the strength level instead of tensile strength. This seems to be reasonable as the bending failure occurs on the convex tensile strained side of the specimen [2]. Such an approach enables to avoid the problems with clamping forces typical for conventional tensile tests. Three rectangular plates $50 \times 10 \times 3 \text{ mm}^3$ have been cut from each composite sample in the longitudinal direction to be bend strained in ZWICK Z100 apparatus with a cross-head rate of 1 mm min^{-1} . The composites Mg₂Li/T300 and Mg₂Li/Granoc have been 3-point bend strained. Both the bending strength and Young's modulus have been calculated from load vs bend displacement diagrams using standard procedures [10].

3. Results and discussion

3.1. Composite structure

Figures 1a,b show the overall distribution of T300 and Granoc carbon fibres ($\sim 45 \text{ vol. } \%$) within Mg₂Li

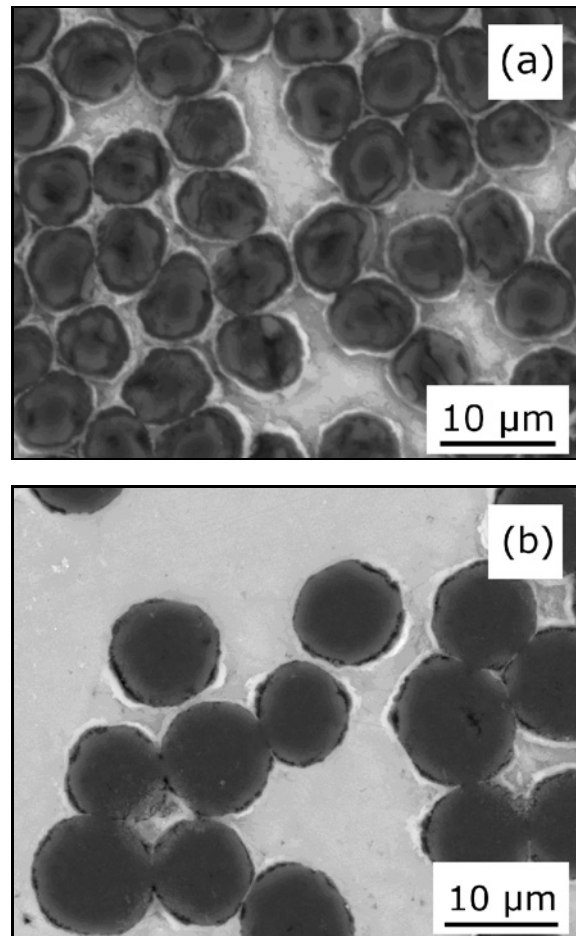


Fig. 2. Morphology of cross-sections of T300 (a) and GRANOC (b) carbon fibres in Mg₂Li matrix (BSE).

matrix, respectively. Since the fibres have been inserted into fibrous preform relatively loosely, inhomogeneity in the fibre distribution (fibres free regions) occurs between individual yarns. Morphology of cross-sections of T300 and Granoc carbon fibres in Mg₂Li matrix is shown in Figs. 2a and 2b, respectively. No precipitation takes place in the matrix region as Mg-Li alloys up to $\sim 5.2 \text{ wt. } \%$ Li are based on homogeneous h.c.p. solid solution structure [11]. There are recognizable in some cases bright regions surrounding individual fibres which can be attributed to Li segregation. Higher Li content around the fibres makes Mg-Li alloys prone to the reaction with air humidity producing LiOH. This hydroxide layer disappears after sputtering.

3.1.1. Auger analysis

The aim of Auger electron spectroscopy analysis is to verify the presumption that oxidic compound occurrence on the cross-section of carbon fibres is lithium hydroxide LiOH formed by the hydrolytic decomposi-

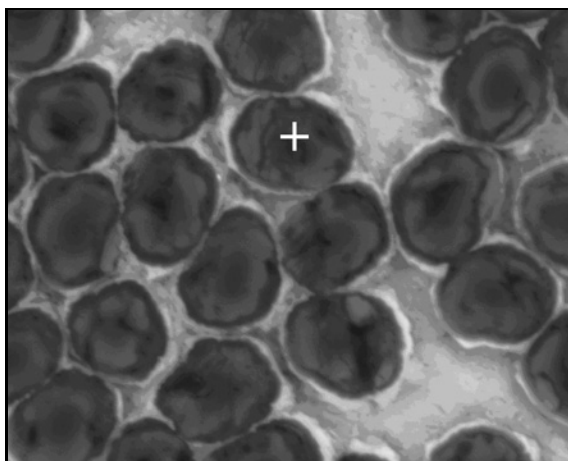


Fig. 3. Cross-section of T300 carbon fibres illustrating the position of point Auger analysis.

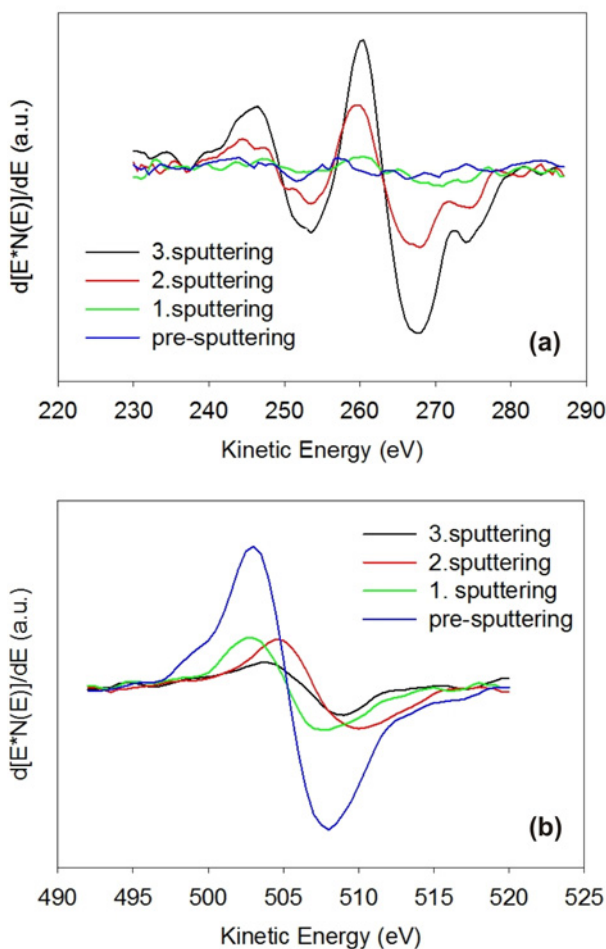


Fig. 4. Auger spectra sequences obtained simultaneously in the kinetic energy windows of 230–290 eV (a) and 490–520 eV (b) including respectively “carbodic” C(KVV) and “oxidic” O(KVV) Auger transitions.

tion of Li_2C_2 with air humidity:



For that purpose, the Auger spectra were taken gradually from the same point on the cross-section of the same carbon fibre in MgLi/T300 composite (Fig. 3). Figures 4a,b show Auger spectra sequences obtained simultaneously in the kinetic energy windows of 230–290 eV and 490–520 eV including respectively “carbodic” C(KVV) and “oxidic” O(KVV) Auger transitions. In the initial state (pre-sputtering), there has been detected strong O(KVV) peak at 508 eV (Fig. 4b) and no C(KVV) peak (Fig. 4a). Several subsequent recording + sputtering steps have generated C(KVV)/O(KVV) spectra sequences which indicate gradual evolution of C(KVV) peak at 268 eV (Fig. 4a) and the simultaneous disappearance of O(KVV) peak at 508 eV (Fig. 4b). In the final stage, there have been obtained well developed C(KVV) patterns characterized by the peak doublet at 254 and 268 eV and a small residue of O(KVV) signal at 508 eV. This C(KVV) patterns doublet coincides exactly with that reported for Li_2C_2 formed on lithium film after being exposed to acetylene [12]. Hence, the above described Auger analysis clearly confirms that the oxidic layer (LiOH) on lithium affected T300 carbon fibres has been formed on Li_2C_2 substrate.

3.1.2. EDX analysis

Auger analysis has provided evidence that some oxidic compound has been formed on Li_2C_2 substrate on CF cross-section. This oxidic compound is considered lithium hydroxide LiOH produced by hydrolysis of Li_2C_2 via Eq. (1). It is plausible to presume that a specific correlation exists between the amount of Li_2C_2 on the fibre cross-section and amount of LiOH formed. Accordingly, we have taken the EDX determined oxygen concentration on the fibre cross-section as a rough indication of Li_2C_2 amount. Before the EDX analysis, each metallographically prepared sample has been exposed to air at room temperature for the same time (~ 1 h).

Table 2 shows EDX detected oxygen concentrations on the cross-section of the fibre of Mg2Li/T300 composites infiltrated at 700 °C for different times. Oxygen concentration represents a mean value of five $\text{OK}\alpha$ signals (point measurement) taken from the central part of arbitrarily selected fibre cross-sections in a given composite. It is seen that there exists some correlation between the oxygen content and the infiltration times. It is also seen that oxygen content grows rapidly with infiltration time, thus demonstrating rapid kinetics of Li_2C_2 formation inside the carbon fibres.

Figures 5–7 show SEM micrographs of the struc-

Table 2. Bending strength and Young's modulus values of Mg/T300, Mg₂Li/T300, Mg/Granoc, and Mg₂Li/Granoc composites (3-point bend test)

Composite	Infiltration		Oxygen (wt.%)	Bending strength (MPa)	Young's modulus (GPa)
	T (°C)	t (s)			
Mg/T300	700	60	0.11	867	99
Mg ₂ Li/T300	700	5	3.26	1210	109
Mg ₂ Li/T300	700	15	6.20	1086	103
Mg ₂ Li/T300	700	30	8.88	1075	109
Mg ₂ Li/T300	700	60	18.53	769	112
Mg/Granoc	750	120	–	584	180
Mg ₂ Li/Granoc	750	30	0.21	579	190
Mg ₂ Li/Granoc	750	60	30.8	522	150
Mg ₂ Li/Granoc	850	30	8.64	546	177
Mg ₂ Li/Granoc	850	60	44.02	525	168

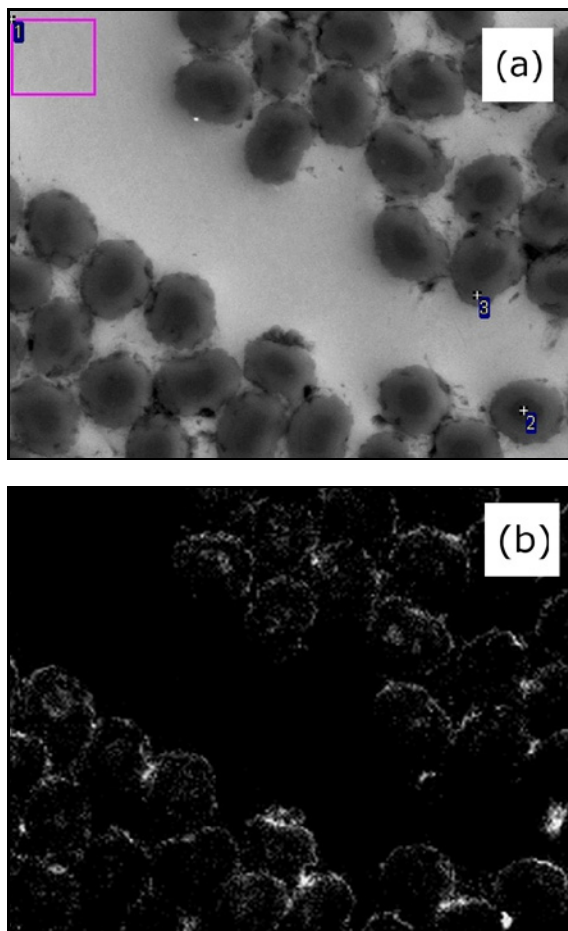


Fig. 5. BSE image of the structure of Mg₂Li/T300 composite infiltrated at 700 °C/5 s (a) and corresponding EDX map of OK α distribution (b). Local oxygen concentrations at labelled sites: 1 – 0.62 wt.%, 2 – 4.66 wt.%, and 3 – 3.59 wt.%.

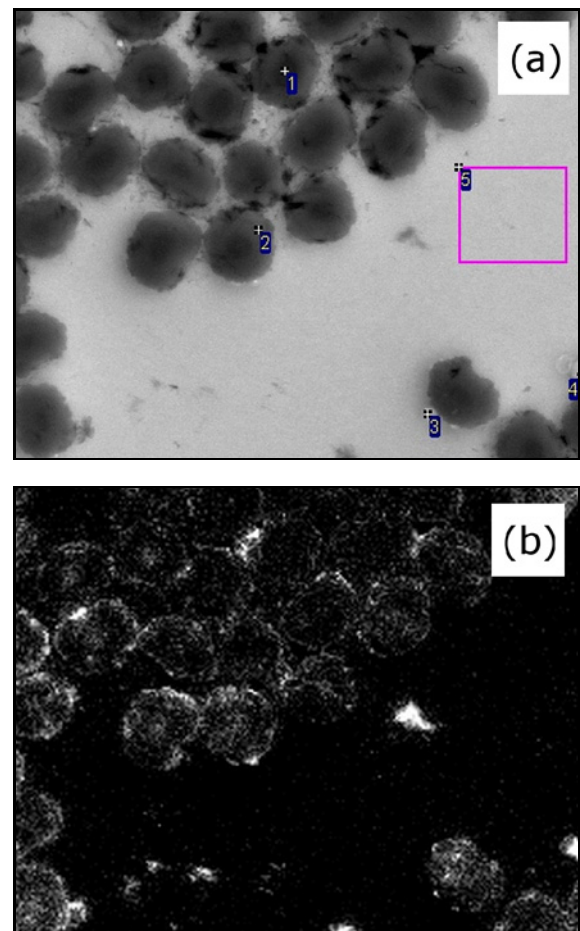


Fig. 6. BSE image of the structure of Mg₂Li/T300 composite infiltrated at 700 °C/15 s (a) and EDX map of OK α distribution (b). Local oxygen concentrations at labelled sites: 1 – 5.89 wt.%, 2 – 6.51 wt.%, 3 – 1.28 wt.%, 4 – 11.43 wt.%, and 5 – 0.51 wt.%.

ture of Mg₂Li/T300 composites and corresponding EDX maps of oxygen distribution as well as local oxy-

gen concentrations at labelled sites (OK α signal). The composites have been infiltrated at 700 °C for differ-

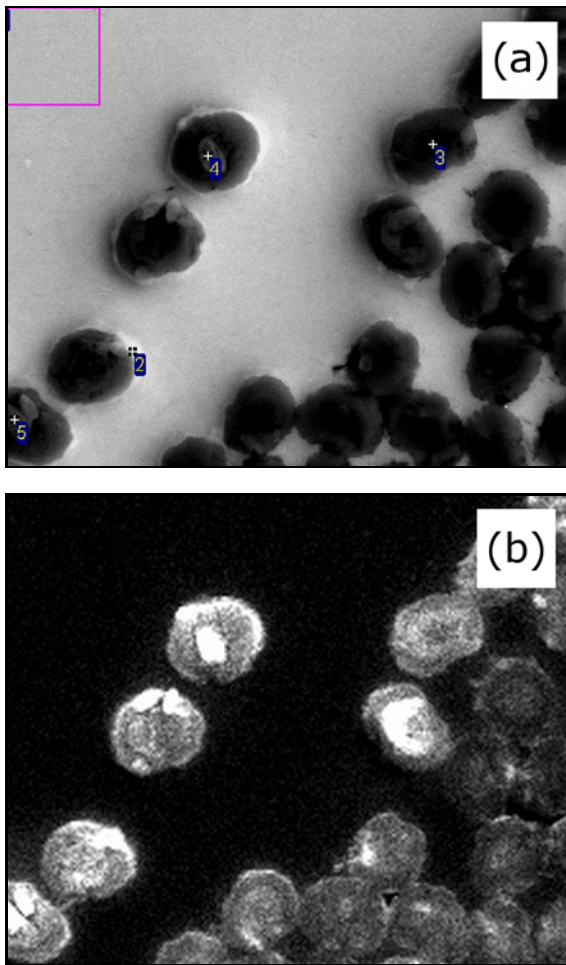


Fig. 7. BSE image of the structure of Mg₂Li/T300 composite infiltrated at 700 °C/60 s (a) and EDX map of OK α distribution (b). Local oxygen concentrations at labelled sites: 1 – 0.71 wt.%, 2 – 14.77 wt.%, 3 – 16.43 wt.%, 4 – 19.26 wt.%, and 5 – 21.29 wt.%.

ent times (5, 15, and 60 s), and presented EDX results demonstrate progress in the reaction of carbon fibres with Li. Figure 5 corresponds to very early infiltration stage (5 s), and it is seen that a thorough fibres attack has occurred despite short infiltration time. Weak OK α signal is distributed irregularly on the fibre cross-sections wherein ring-shaped oxygen-enriched zone occurs at the periphery of the fibres. Similar nature of the oxygen distribution can also be observed in composites infiltrated for a longer time (15 s), but OK α signal is significantly stronger (Fig. 6). Further prolongation of infiltration time (60 s) results in strongly enhanced oxygen concentration and non-uniform oxygen distribution over the cross-section area (Fig. 7).

Pitch-based carbon fibres Granoc are expected to be more stable against lithium attack due to their more ordered graphitic structure. Figure 8 shows the SEM image and the map of OK α signal in Mg₂Li/Granoc composite prepared at 750 °C/30 s.

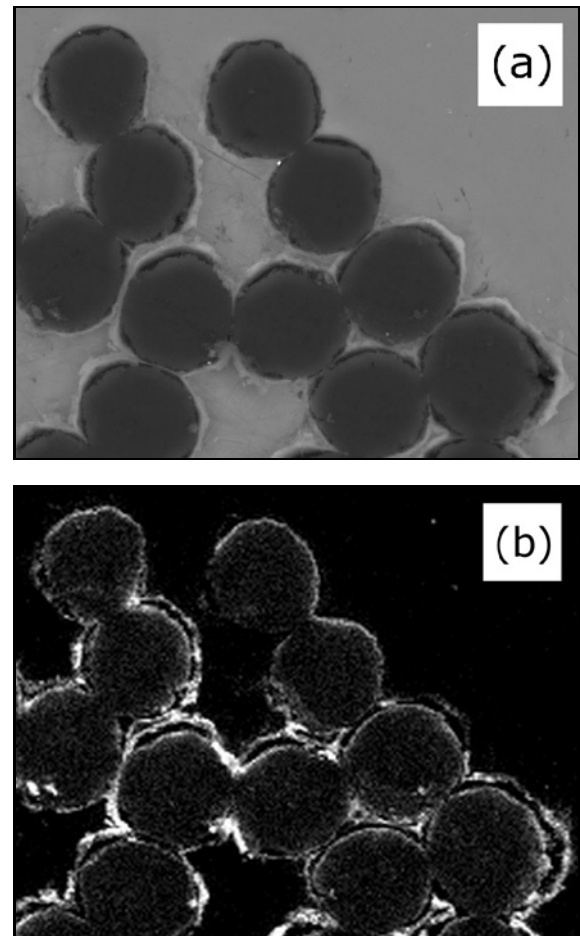


Fig. 8. BSE image (a) and EDX map of OK α signal (b) of Mg₂Li/GRANOC composite infiltrated at 750 °C/30 s.

SEM image and OK α map demonstrate that individual fibres are surrounded by bright zones that are enriched with oxygen. We consider them the signs of lithium segregation around the fibre surfaces. At the same time, practically no OK α signal occurs inside the fibres, thus indicating that Granoc fibres are resistant to lithium attack under given infiltration conditions. Hence, lithium atoms appear to be accumulated outside the Granoc fibres and are not able to penetrate the interior of the fibres.

By contrast, infiltration of Granoc fibres at 850 °C/30 s results in thorough penetration of lithium inside the fibres as manifested by strong and fairly uniform OK α signal within the whole fibre cross-section (Fig. 9). Quantitative EDX data show that oxygen occurs there at the concentration level of 7–8 wt.%. It is also seen those bright regions around the fibres that are considered the signs of Li segregation are entirely missing, which suggests that Li has been wholly consumed with carbon fibres.

Very high oxygen concentration has been detected on fibres cross-sections in composites infiltrated at 750 °C/60 s and 850 °C/60 s which suggests that there

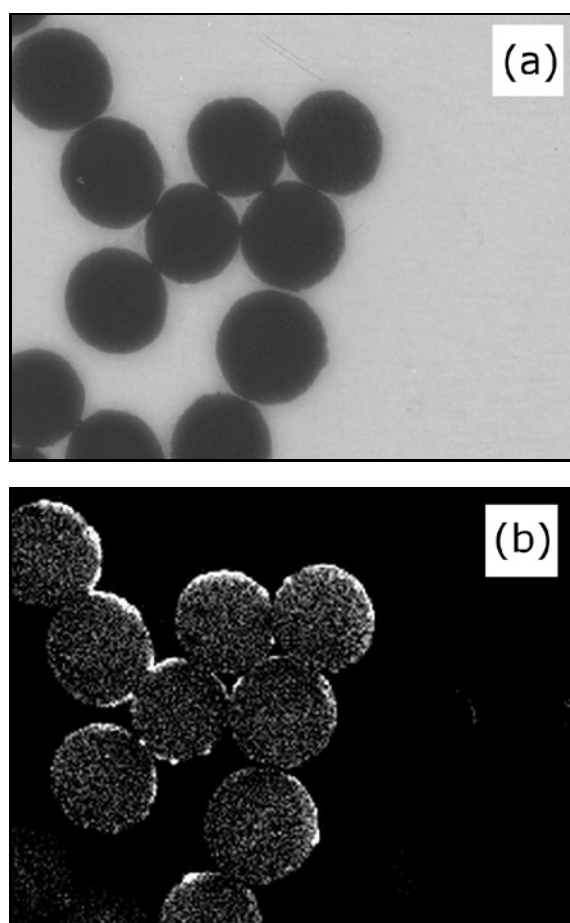


Fig. 9. BSE image (a) and EDX map of $OK\alpha$ signal (b) of $Mg_2Li/GRANOC$ composite infiltrated at $850^\circ C/30$ s.

exist diffusion pathways enabling Li to occupy whole fibre bulk within several tens of seconds. Considering the ordered graphitic structure of Granoc carbon fibres, such fast diffusion tracks for Li atoms might be, e.g., the spaces between graphene hexagons. Taking into account very high interplanar mobility of Li in turbostratic carbon ($D \approx 10^{-7} \text{ cm}^2 \text{ s}^{-1}$ at 1000 K [13]) and small fibre radius ($\sim 5 \mu\text{m}$) lithium should be able to saturate whole fibre volume already within few seconds. Nevertheless, the main energetic barrier is apparently connected with an escape of Li atoms from MgLi melt into interplanar spaces of the graphitic structure.

3.2. Bending tests

3-point bending test has been used to evaluate the effect of Li reaction with carbon fibres on the strengthening in $Mg_2Li/T300$ composites infiltrated at $700^\circ C$. Oxygen concentration data acquired by EDX from the fibre cross-section areas indicate that Li_2C_2 formation increases monotonously with prolongation of infiltration time.

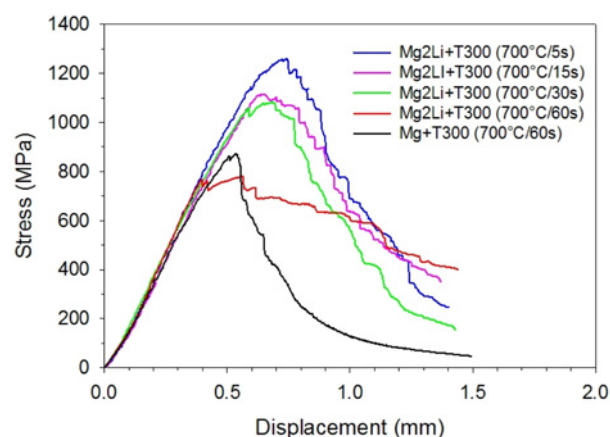


Fig. 10. Representative stress-displacement curves of $Mg/T300$ and $Mg_2Li/T300$ composites infiltrated at $700^\circ C$ for different time (3-point bending test).

The bending strengths and E -modulus data of composites studied as calculated from load-deflection diagrams for different infiltration times (5–60 s) are listed in Table 2. Representative load-deflection curves demonstrate a rapid drop in bending strength with prolonged infiltration time (Fig. 10). The resultant strengthening effect is apparently governed with an interplay between improving interfacial bond and damage of carbon fibres due to Li attack. Accordingly, the favourable impact of Li alloying on the interfacial strength is limited to the very short contact time, and then the degradation phenomena linked with Li_2C_2 formation become dominating. Formation of carbidic phase is, however, adverse to the composite. The creation of carbides consumes C atoms of the carbon fibre, thus breaking the original structure of the fibre, which would significantly degenerate the fibre properties [14, 15]. The orthorhombic crystal structure was reported for Li_2C_2 at room temperature that transforms to cubic at about $500^\circ C$ [16, 17]. As Li_2C_2 is structurally incoherent with the turbostratic graphitic structure of PAN-based T300 fibres, its accumulation inside carbon fibres causes their degradation. Excessive Li_2C_2 production may, therefore, be a reason for lower strengthening efficiency of carbon fibres in Mg_2Li matrix composites infiltrated for a longer time.

Compared with unalloyed $Mg/T300$ composites a remarkable strengthening (by $\sim 35\%$) has been reached particularly in $Mg_2Li/T300$ composites infiltrated for a short time (5 s). Further prolongation of infiltration time up to 60 s has to lead to a remarkable decrease in bending strength of $Mg_2Li/T300$ composites even below the level of unalloyed Mg-based composites. Bending curves in their linear section exhibit roughly similar slope, which is indicative of little differences in Young's modulus of composites tested. However, a slight growing tendency with prolonged in-

filtration time is recognizable (Table 2). Provided that interfacial bond is perfect the stress-strain response of unidirectional long fibre reinforced composites should be governed with deformation behaviour of reinforcing carbon fibres, i. e., it should be linear up to composite failure. Carbon fibres affect the strengthening of magnesium matrix composite tremendously as they undertake most of the load from external loading [14]. When neglecting some non-linearities at the straining beginning, the departure from linearity can be ascribed mainly to the fibres damage and/or insufficient stress sharing at interfaces [18].

The bend straining tests have also been conducted with Mg₂Li/Granoc composites infiltrated at 750 °C and 850 °C for 30 and 60 s. Owing to more ordered graphitic structure the pitch-based Granoc fibres are expected to be more resistant to Li attack than PAN-based T300 ones. The above-reported EDX analysis (OK α signal) has confirmed this assumption only for Mg₂Li/Granoc composites infiltrated at 750 °C/30 s (Fig. 8). On the other hand, considerable affection of Granoc fibres has occurred in composites infiltrated at 850 °C/30 s (Fig. 9) and very strong Li attack has also been observed in composites infiltrated at 750 °C/60 s and 850 °C/60 s. Bending strengths and Young's moduli of Mg/Granoc and Mg₂Li/Granoc composites are listed in Table 2 in dependence on infiltration parameters (temperature, time). Representative stress vs deflection curves of Mg₂Li/Granoc and Mg/Granoc composites are shown in Fig. 11. Except for Mg₂Li/Granoc composite infiltrated at 750 °C/30 s, bending strengths of other Mg₂Li/Granoc composites are well below the strength of Mg/Granoc ones. It is also seen that the strength level of Mg/Granoc and Mg₂Li/Granoc composites is much lower than that of Mg/T300 and Mg₂Li/T300 composites for the same fibre fraction (~ 45 vol.%). This is a somewhat surprising finding as the tensile strengths of Granoc and T300 fibres are nearly the same (3.50 and 3.53 GPa, respectively). Hence, lithium addition to Mg matrix does not improve interfacial strength in Mg₂Li/Granoc composites. While the bending strength of Mg₂Li/T300 composites is susceptible to infiltration temperature-time regime (Fig. 10), Mg₂Li/Granoc ones exhibit only little response to the change in infiltration parameters as demonstrated by small differences in bend straining curves (Fig. 11). Extensive formation of Li₂C₂ observed in Mg₂Li/Granoc composites infiltrated for 60 s resulted in a relatively small decrease in bending strength.

Young's moduli of Mg₂Li/Granoc composites differ only little from each other and are nevertheless considerably higher than those of Mg₂Li/T300 composites. This observation agrees with expectations as Young's modulus of Granoc fibres (860 GPa) is much higher than that of T300 fibres (230 GPa). However,

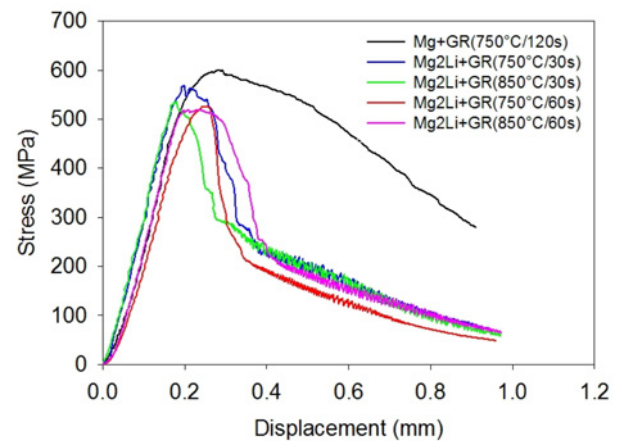


Fig. 11. Representative stress – displacement curves of Mg/GRANOC and Mg₂Li/GRANOC composites for different temperature-time infiltration regimes (3-point bending test).

experimental Young's moduli of Mg₂Li/Granoc composites are far lower than the values calculated using the rule of mixture (411 GPa). This suggests that the strengthening potential of Granoc fibres in Mg₂Li matrix has not been reached. For comparison, Young's moduli of Mg₂Li/T300 composites are quite close to the rule of mixture value (128 GPa).

4. Conclusions

Mg-2 wt.% Li matrix composites unidirectionally reinforced with T300 and Granoc carbon fibres (~ 45 vol.%) have been prepared by gas pressure infiltration technique. There has been studied the interaction of carbon fibres with MgLi melt and its effect on the structure and bending strength of composites prepared. Results obtained are as follows:

1. During the infiltration of T300 and Granoc carbon fibres with Mg-2 wt.% Li alloy lithium penetrates inside the fibres to form Li₂C₂. Presence of Li₂C₂ on fibres cross-section has been detected by Auger electron spectroscopy. Progress in Li₂C₂ formation has been monitored by EDX as OK α signal generated by LiOH from Li₂C₂ hydrolysis.

2. Infiltration of PAN-based T300 carbon fibres with molten Mg-2 wt.% Li alloy has been performed at 700 °C for different time (5, 15, 30, and 60 s). Lithium alloying facilitates the wetting of carbon fibres and at the same time causes their damage through Li₂C₂ formation. Maximum bending strength (1210 MPa) has been reached in composites infiltrated for shortest time (5 s) and then falls monotonously down with prolongation of infiltration time (up to 60 s).

3. Pitch-based Granoc carbon fibres have been infiltrated with Mg-2 wt.% Li alloy at 750 °C and 850 °C

for 30 s and 60 s. Lithium alloying of Mg matrix does not show any decisive role in composite strengthening so that the strengthening efficiency of Granoc fibres is much lower compared to that of T300 fibres. For the same fibre fraction, the bending strength of Mg/T300 and Mg₂Li/T300 composites is mostly higher than that of Mg/Granoc and Mg₂Li/Granoc composites.

Acknowledgement

Grant Agency of the Slovak Republic VEGA is acknowledged for supporting this work (Project No 2/0144/17).

References

- [1] K. Shirvanimoghaddam, S. U. Hamim, M. K. Akbari, S. M. Fakhrohsein, H. Khayyam, A. H. Pakseresht, E. Ghasali, M. Zabet, K. S. Munir, S. Jia, J. P. Davim, M. Naebe, Carbon fibre reinforced metal matrix composites: Fabrication processes and properties, *Composites A* 92 (2017) 70–96. [doi:10.1016/j.compositesa.2016.10.032](https://doi.org/10.1016/j.compositesa.2016.10.032)
- [2] C. Körner, W. Schäff, M. Otmüller, R. F. Singer, Carbon long fiber reinforced magnesium alloys, *Adv. Eng. Mater.* 2 (2000) 327–337. [doi:10.1002/1527-2648\(200006\)2:6<327::AID-ADEM327>3.0.CO;2-W](https://doi.org/10.1002/1527-2648(200006)2:6<327::AID-ADEM327>3.0.CO;2-W)
- [3] A. Feldhoff, E. Pippel, J. Woltersdorf, Interface engineering of carbon-fiber reinforced Mg-Al alloys, *Adv. Eng. Mater.* 2 (2000) 471–480. [doi:10.1002/1527-2648\(200008\)2:8<471::AID-ADEM471>3.0.CO;2-S](https://doi.org/10.1002/1527-2648(200008)2:8<471::AID-ADEM471>3.0.CO;2-S)
- [4] S. F. Zhang, G. Q. Chen, R. S. Pei, Y. P. Wang, D. G. Li, P. P. Wang, G. H. Wu, Effect of Y content on interfacial microstructures and mechanical properties of Cf/Mg composite, *Mater. Sci. Eng. A* 647 (2015) 105–112. [doi:10.1016/j.msea.2015.08.076](https://doi.org/10.1016/j.msea.2015.08.076)
- [5] S. F. Zhang, G. Q. Chen, R. S. Pei, M. Hussain, Y. P. Wang, D. G. Li, P. P. Wang, G. H. Wu, Effect of Gd content on interfacial microstructures and mechanical properties of Cf/Mg composite, *Materials & Design* 65 (2015) 567–574. [doi:10.1016/j.matdes.2014.09.045](https://doi.org/10.1016/j.matdes.2014.09.045)
- [6] S. Kúdela Jr., O. Bajana, L. Orovčík, Z. Ranachowski, P. Ranachowski, Alloying effect of Li and Y on the strengthening of Mg/T300 composites, *Kovove Mater.* 58 (2020) 151–159. [doi:10.4149/km.2020_3_151](https://doi.org/10.4149/km.2020_3_151)
- [7] X. Qin, Y. Lu, H. Xiao, Y. Wen, T. Yu, A comparison of the effect of graphitization on microstructures and properties of polyacrylonitrile and mesophase pitch-based carbon fibers, *Carbon* 50 (2012) 4459–4469. [doi:10.1016/j.carbon.2012.05.024](https://doi.org/10.1016/j.carbon.2012.05.024)
- [8] Torayca Data Sheet, Tokio, Toray Industries Inc., 2011.
- [9] Granoc Yarn XN Series, Nippon Graphite Fiber Corporation, www.ngfworld.com
- [10] F. Pišek, *Material Science II*, Nakladatelství ČSAV, Praha, 1959. (in Czech)
- [11] R. E. Lee, W. J. D. Jones, Microplasticity and fatigue of some magnesium-lithium alloys, *Mater. Sci.* 9 (1974) 469–475. [doi:10.1007/BF00737849](https://doi.org/10.1007/BF00737849)
- [12] S. M. Gates, H. M. Meyer, L. G. Pedersen, G. C. Jarnagin, Electronic and geometric structure of acetylide carbon on the surface of lithium, *Surface Science* 140 (1984) 455–471. [doi:10.1016/0039-6028\(84\)90746-5](https://doi.org/10.1016/0039-6028(84)90746-5)
- [13] B. Jungblut, E. Hoinkis, U. Doebler, H. L. Meyerheim, The diffusion of Li in Poco graphite and glassy carbon at low concentrations and high temperatures, *Berichte Bunsen. Phys. Chem.* 93 (1989) 1317–1322. [doi:10.1002/bbpc.19890931135](https://doi.org/10.1002/bbpc.19890931135)
- [14] L. Qi, S. Li, T. Zhang, J. Zhou, H. Li, An analysis of the factors affecting strengthening in carbon fiber reinforced magnesium composites, *Composite Structures* 209 (2019) 328–336. [doi:10.1016/j.compstruct.2018.10.109](https://doi.org/10.1016/j.compstruct.2018.10.109)
- [15] S. Li, L. Qi, T. Zhang, J. Zhou, H. Li, Interfacial microstructure and tensile properties of carbon fiber reinforced Mg-Al-RE matrix composites, *J. of Alloys & Comp.* 663 (2016) 686–692. [doi:10.1016/j.jallcom.2015.12.165](https://doi.org/10.1016/j.jallcom.2015.12.165)
- [16] J. Sangster, C-Li (Carbon-Lithium) system, *J. Phase Equilib. Diff.* 28 (2007) 561–570. [doi:10.1007/s11669-007-9193-8](https://doi.org/10.1007/s11669-007-9193-8)
- [17] U. Ruschewitz, R. Pöttgen, Structural phase transition in Li₂C₂, *Zeitschr. Anorg. Allg. Chem.* 625 (1999) 1599–1603. [doi:10.1002/\(SICI\)1521-3749\(199910\)625:10<1599::AID-ZAAC1599>3.0.CO;2-J](https://doi.org/10.1002/(SICI)1521-3749(199910)625:10<1599::AID-ZAAC1599>3.0.CO;2-J)
- [18] Y. Wang, L. Jiang, R. Pei, G. Chen, X. Lin, M. Song, G. Wu, Effect of long-period-stacking-ordered phases on the microstructure and mechanical properties of carbon fiber reinforced magnesium gadolinium-zinc composite, *J. Alloys & Comp.* 708 (2017) 728–733. [doi:10.1016/j.jallcom.2017.03.045](https://doi.org/10.1016/j.jallcom.2017.03.045)
- [19] Z. L. Pei, K. Li, J. Gong, N. L. Shi, E. Elangovan, C. Sun, Micro-structural and tensile strength analyses on the magnesium matrix composites reinforced with coated carbon fiber, *J. Mater. Sci.* 44 (2009) 4124–4131. [doi:10.1007/s10853-009-3604-7](https://doi.org/10.1007/s10853-009-3604-7)
- [20] L. Ju, L. Qi, X. Wei, J. Zhou, X. Hou, H. Li, Damage mechanism and progressive failure analysis of Cf/Mg composite, *Mater. Sci. Eng. A* 666 (2016) 257–263. [doi:10.1016/j.msea.2016.04.067](https://doi.org/10.1016/j.msea.2016.04.067)